HAL
archives-ouvertes.fr

Shape From Shading

Emmanuel Prados, Olivier Faugeras

▶ **To cite this version:**

Emmanuel Prados, Olivier Faugeras. Shape From Shading. N. Paragios, Y. Chen and O. Faugeras. Handbook of Mathematical Models in Computer Vision, Springer, pp.375–388, 2006, 978-0387263717. inria-00377417

HAL Id: inria-00377417
https://hal.inria.fr/inria-00377417

Submitted on 21 Apr 2009

HAL is a multi-disciplinary open access archive for the deposit and dissemination of scientific research documents, whether they are published or not. The documents may come from teaching and research institutions in France or abroad, or from public or private research centers.

L'archive ouverte pluridisciplinaire **HAL**, est destinée au dépôt et à la diffusion de documents scientifiques de niveau recherche, publiés ou non, émanant des établissements d'enseignement et de recherche français ou étrangers, des laboratoires publics ou privés.

Shape From Shading

Emmanuel Prados, Olivier Faugeras

ABSTRACT Shape From Shading is the process of computing the three-dimensional shape of a surface from one image of that surface. Contrary to most of the other three-dimensional reconstruction problems (for example, stereo and photometric stereo), in the Shape From Shading problem, data are minimal (we use a single image!). As a consequence, this inverse problem is intrinsically a difficult one. In this chapter we describe the main difficulties of the problem and the most recent theoretical results. We also give some examples of realistic modelings and of rigorous numerical methods.

1 Introduction

The "Shape From Shading" problem (SFS) is to compute the three-dimen-sional shape of a surface from the *brightness* of *one* black and white image of that surface; see figure 1.

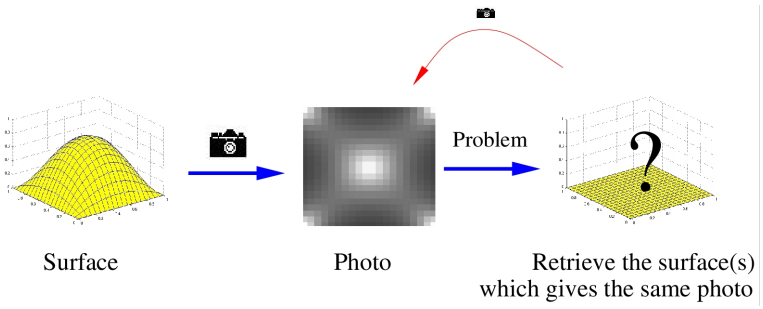

FIGURE 1. The "Shape-from-Shading" problem.

In the 70's, Horn [18] was the first to formulate the Shape From Shading problem simply and rigorously as that of finding the solution of a nonlinear first-order Partial Differential Equation (PDE) called the brightness equation. In a first period (in the 80's) the authors focus on the computational part of the problem, trying to compute directly numerical solutions. Questions about the existence and uniqueness of solutions to the problem were simply not even posed at that time with the important exception of the work of Bruss and Brooks [8, 5]. Nevertheless, due to the poor quality of the results, these questions as well as those related to the convergence of numerical schemes for computing the solutions became central in the last decade of the 20th century. Today, the Shape From Shading problem is

a) b) c)

a) The crater illusion [31]: From the image we perceive two craters, a small and a big one. But we can turn these craters into volcanoes (although upside down) if we imagine the light source to be at the bottom of the picture rather than at the top. This picture is actually that of a pair of ash cones in the Hawaiian Island, not that of a pair of craters. b-c) "Bas-relief Ambiguity" [4]: Frontal and side views of a marble bas-relief sculpture. Notice how the frontal views appear to have full 3-dimensional depth, while the side view reveals the flattening. This demonstrates that the image b) can be produced by two surfaces: the three-dimensional surface we imagine by visualizing image b) and the actual bas-relief which is at the origin of the two photos b) and c).

FIGURE 2. Examples of Shape From Shading ambiguities.

known to be an ill-posed problem. For example, a number of articles show that the solution is not unique [5, 28, 29, 38, 4, 16, 36, 34]. The encountered difficulties have often been illustrated by such concave/convex ambiguities as the one displayed in Figure 2-a). In this figure, the ambiguity is due to a change of the estimation of the parameters of the lighting. In fact, this kind of ambiguity can be widely generalized. In [4], Belhumeur and colleagues prove that when the lighting direction[1] and the Lambertian reflectance (albedo) of the surface are unknown, then the same image can be obtained by a continuous family of surfaces (depending linearly of three parameters). In other words, they show that neither shading nor shadowing of an object, seen from a single viewpoint reveals its exact 3D structure. This is the "Bas-relief Ambiguity", see [4] and Figures 2-b) and 2-c). Being aware of these difficulties, we therefore assume here that all the parameters of the light source, the surface reflectance and the camera are known.

As we have mentioned above, the modeling of the Shape From Shading problem introduced by Horn leads to a PDE: the brightness equation. This equation arises from the following

$$I(x_1, x_2) = R(\mathbf{n}(x_1, x_2)),$$

(x_1, x_2) are the coordinates of a point x in the image. The brightness equation connects the reflectance map (R) to the brightness image (I). At the exception of an extremely small number of papers, for example [1, 25, 37],

[1] In the case of a distant light source.

almost all the Shape From Shading methods assume that the scene is Lambertian. In this case, the reflectance map is the cosine of the angle between the light vector $\mathbf{L}(x)$ and the normal vector $\mathbf{n}(x)$ to the surface:

$$R = \cos(\mathbf{L}, \mathbf{n}) = \frac{\mathbf{L}}{|\mathbf{L}|} \cdot \frac{\mathbf{n}}{|\mathbf{n}|}, \tag{1.1}$$

(where R, $\mathbf{L}$ and $\mathbf{n}$ depend on (x_1, x_2)).

2 Mathematical formulation of the SFS problem

In this section, we formulate the SFS problem as that of solving some explicit PDEs. These explicit equations arise from equations (1.1).
Let Ω be an open subset of $\mathbb{R}^2$ representing the image domain (e.g. the rectangle $]0, X[\times]0, Y[$). We represent the scene by a three-dimensional surface $\mathfrak{S} = \left\{S(x);\ x \in \overline{\Omega}\right\}$, which can be explicitly parameterized by using the function S defined on the closure $\overline{\Omega}$ into $\mathbb{R}^3$. The particular type of parameterization is irrelevant here but may vary according to the camera type (orthographic versus pinhole) and to mathematical convenience. In this work, we assume that the light source is unique and punctual. For $y \in \mathbb{R}^3$, we denote $\mathbf{L}(y)$ the *unit* vector representing the light source direction at the point y. If the light source is located at infinity then the light vector field is uniform (i.e. constant). In this case, we denote by $\mathbf{L} = (\alpha, \beta, \gamma)$ with $\gamma > 0$, and $\mathbf{l} = (\alpha, \beta)$. If the light source is located at the optical center, then $\mathbf{L}(S(x)) = S(x)/|S(x)|$.

2.1 "Orthographic SFS" with a far light source

This is the traditional setup for the SFS problem. Here, we assume in particular that the camera performs an orthographic projection of the scene. For such a modeling, it is natural to denote by u the *distance* of the points in the scene to the camera; in other words, $\mathfrak{S}$ is parameterized by $S : x \mapsto (x, u(x))$. For such a parameterization, a normal vector $\mathbf{n}(x)$ at the point $S(x)$ is given by[2] $\mathbf{n}(x) = (-\nabla u, 1)$. The SFS problem is then, given I and $\mathbf{L}$, to find a function $u : \overline{\Omega} \longrightarrow \mathbb{R}$ satisfying the brightness equation:

$$\forall x \in \Omega, \quad I(x) = (-\nabla u(x) \cdot \mathbf{l} + \gamma)/\sqrt{1 + |\nabla u(x)|^2}.$$

In the SFS literature, this equation is rewritten in a variety of ways as $H(x, p) = 0$, where $p = \nabla u$. For example, Rouy and Tourin [38] introduce

$$H_{R/T}(x, p) = I(x)\sqrt{1 + |p|^2} + p \cdot \mathbf{l} - \gamma.$$

[2] The two columns of the Jacobian $DS(x)$ are tangent vectors to $\mathfrak{S}$ at the point $S(x)$. Their cross product is a normal vector.

In [14], Dupuis and Oliensis consider

$$H_{D/O}(x,p) = I(x)\sqrt{1+|p|^2-2p\cdot\mathbf{l}}+p\cdot\mathbf{l}-1.$$

In the case where $\mathbf{L}=(0,0,1)$, Lions et al. [26] deal with:

$$H_{Eiko}(x,p) = |p| - \sqrt{\tfrac{1}{I(x)^2}-1}. \qquad \text{(called the Eikonal equation).}$$

The function H is called the *Hamiltonian*.

2.2 "Perspective SFS" with a far light source

"Perspective SFS" assumes that the camera performs a perspective projection of the scene. We therefore assume that $\mathfrak{S}$ can be explicitly parameterized by the *depth modulation* function u defined on $\overline{\Omega}$. In other words, we choose $S(x) = u(x).(x,-f)$, $\forall x \in \overline{\Omega}$, where f denotes the focal length. For such a parameterization, a normal vector $\mathbf{n}(x)$ at the point $S(x)$ is given by[2] $\mathbf{n}(x) = (f\nabla u(x), u(x) + x\cdot\nabla u(x))$. Combining the expression of $\mathbf{n}(x)$ and the change of variables[3] $v = ln(u)$, we obtain from the irradiance equation (1.1) the following Hamiltonian [34, 41, 11]:

$$H_{P/F}(x,p) = I(x)\sqrt{f^2|p|^2+(x\cdot p+1)^2}-(f\ \mathbf{l}+\gamma x)\cdot p-\gamma;$$

2.3 "Perspective SFS" with a point light source at the optical center

Here, we parameterize $\mathfrak{S}$ by $S(x) = u(x)\frac{f}{\sqrt{|x|^2+f^2}}\ (x,-f)$, $\forall x \in \overline{\Omega}$. In this case, we can choose[2] $\mathbf{n}(x) = (f\nabla u - \frac{fu(x)}{|x|^2+f^2}\ x\ ,\ \nabla u\cdot x + \frac{fu(x)}{|x|^2+f^2}\ f)$. Combining the expression of $\mathbf{n}(x)$ and the change of variables[3] $v = ln(u)$, we obtain from equation (1.1) the following Hamiltonian [35, 33]:

$$H_{OptC}(x,p) = I(x)\sqrt{f^2|p|^2+(p\cdot x)^2+Q(x)^2}-Q(x).$$

2.4 A generic Hamiltonian

In [35, 33], Prados and Faugeras proved that all the previous SFS Hamiltonians are special cases of the following "generic" Hamiltonian:

$$H_g(x,p) = \kappa_x\sqrt{|A_x p+\mathbf{v}_x|^2+K_x^2}+\mathbf{w}_x\cdot p+c_x,$$

with $\kappa_x, K_x \geq 0$, $c_x \in \mathbb{R}$, $\mathbf{v}_x, \mathbf{w}_x \in \mathbb{R}^2$ and $A_x \in \mathcal{M}_2(\mathbb{R})$, the set of 2×2 real matrices. They also showed that this "generic" Hamiltonian can be rewritten as a supremum:

$$H_g(x,p) = \sup_{a\in\bar{B}_2(0,1)}\{-f_g(x,a)\cdot p - l_g(x,a)\};$$

[3] We assume that the surface is visible (in front of the retinal plane) hence $u>0$.

see [33] for the detailed expressions of f_g and l_g. This generic formulation considerably simplifies the analysis of the problem. Theorems about the characterization and the approximation of the solutions are proved as much as possible for this generic SFS Hamiltonian. In particular, this formulation *unifies the orthographic and perspective* SFS problems. Also, from a practical point of view, *a single algorithm can be used to numerically solve these various problems.*

3 Mathematical study of the SFS problem

3.1 Related work

It is well-known that the SFS problem is an ill-posed problem even when we assume complete control of the experimental setup. For example, the previous SFS PDEs do not have a unique solution: several surfaces can yield the same image [16]. Before computing a numerical solution, it is therefore very important to answer the following questions. Does there exist a solution? If yes, in what sense is it a solution (classical or weak)? Is the solution unique? The various approaches for providing answers to these questions can be classified in two categories. **First**, Dupuis and Oliensis [14] and Kozera [24] deal with smooth (classical) solutions. More precisely, Dupuis and Oliensis [14] prove the uniqueness of some constrainted C^2 solutions, and they characterize some C^1 solutions. Kozera works with hemi-spheres and planes [24]. Nevertheless, we can design smooth images "without (smooth) shape" [6, 23]; also, because of noise, of errors on parameters (focal length, light position, etc) and of incorrect modeling (interrecflections, extended light source, nonlambertian reflectance...) there never exist in practice such smooth solutions with real images. In other respects, this also explains why the global methods (e.g. [14, 20, 27]) which are completely based on such regularity assumptions are somewhat disappointing with real images. This leads to consider the problem in a weaker framework. **Second**, in the 90s, Lions, Rouy and Tourin [38, 26] propose to solve the SFS problem by using the notion of viscosity solutions. Recently, their approach has been extended by Prados and Faugeras [36, 34] and by Falcone [9]. The theory of viscosity solutions is interesting for a variety of reasons: 1) it ensures the existence of weak solutions as soon as the intensity image is (Lipschitz) continuous; 2) it allows to characterize all solutions; 3) any particular solution is effectively computable. Nevertheless, the work of Lions et al., Prados and Faugeras, Falcone et al. [38, 26, 36, 34, 9] has a very important weakness: the characterization of a viscosity solution and its computation *require* in particular *the knowledge of its values on the boundary of the image*. This is *quite unrealistic* because in practice such values are not known. At the opposite of the work based on the viscosity solutions, Dupuis and Oliensis [14] characterize some C^1 solutions with much less data. In partic-

ular, they do not specify the values of the solution on the boundary of the image. Considering the advantages and the drawbacks of all these methods, Prados et al. [35, 32] propose a *new* class of *weak* solutions which guarantees the existence of a solution[4] in a large class of situations including some where there do not exist smooth solutions. They call these new solutions: "Singular Discontinuous Viscosity Solutions" (SDVS). The notion of SDVS allows to unify the mathematical frameworks proposed in the SFS literature and to generalize the previous main theoretical results.

3.2 Nonuniqueness and characterization of a solution

The results presented in this section are based on the notion of SDVS [35]. Let us recall that the viscosity solutions are solutions in a weak sense and that the classical (differentiable) solutions are particular viscosity solutions. For more details about this notion of weak solutions, we refer the reader to [2]. For an intuitive approach connected to computer vision, see for example [35] and references therein.

Since the CCD sensors have finite size, we assume that Ω is *bounded*. In this case, it is well known that the Hamilton-Jacobi equations of the form $H(x, \nabla u(x)) = 0$, $\forall x \in \Omega$, (and so the SFS equations considered here) do not have a unique viscosity solution [2]. It follows that for characterizing (and for computing) a solution, we need to impose additional constraints. In [35] (but also implicitly, in [14]) it is shown that the idea of state contraints (also called "Soner conditions") provides a more convenient notion of boundary condition than Dirichlet's[5] or Neumann's[6]. The "state contraint" is a boundary condition which is reduced to

$$H(x, u(x), \nabla u(x)) \geq 0 \qquad \text{on } \partial\Omega,$$

in the viscosity sense (see for example [2]). This constraint corresponds to the Dirichlet conditions

$$\forall x \in \partial\Omega, \quad u(x) = \varphi(x) \quad \text{with } \varphi(x) = +\infty,$$

in the viscosity sense. In a sense, completing an equation with state constraints consists in choosing the highest viscosity solution. The interest of the notion of state constraints is twofold: 1) in contrast with the Dirichlet and Neumann boundary conditions, the state constraints do not require any data[7]. 2) the notion of state constraints can be approximately ex-

[4] Corresponding to Dupuis and Oliensis' solution, if one exists.

[5] Dirichlet conditions consists in fixing the values of the solutions.

[6] Neumann conditions consists in fixing the values of the derivatives the solutions.

[7] Dirichlet (respectively, Neumann) boundary conditions require the knowledge of the exact values of the solution (respectively, the exact values of $\nabla u(x) \cdot n(x)$, where $n(x)$ is the unit inward normal vector to $\partial\Omega$ at the point x) on the boundary of the image. In the SFS problem, we rarely have such data at our disposal.

pressed as "$u(x)$ increases when x tends to $\partial\Omega$"; see [35]. So the addition of this constraint provides a relevant solution as soon as the original surface verifies this basic assumption. Let us emphasize that this constraint is in fact not a strong one since, for example, the condition is satisfied as soon as the image to be processed contains an object of interest in front of a background.

The main difficulty encountered when one attempt to solve the SFS equations (described in section 2) is due to the fact that even if we impose Dirichlet or Soner (state constraints) boundary conditions all over the boundary of the image, these constraints are not sufficient for obtaining the uniqueness of the solution. **For characterizing a weak solution (SDVS) or a classical solution (C^1), it is necessary and sufficient to impose (in addition) *Dirichlet constraints* at the *singular points* which are *local "minima"***[8]; at the other points, we just impose state constraints [32]. Let us remind the reader that the set of the *singular points* is $\mathcal{S} = \{\ x \in \Omega \mid I(x) = 1\ \}$. These points are those of maximal intensity[9] and correspond with the points for which the surface normal coincides with the light direction.

Therefore, in practice, to be able to recover the original surface[10], we need to know what are the singular points which are local minima and the height of the surface at all these particular points. In the cases where we do not have this knowledge (unfortunately, we do not have it in practice!), we are unable to recover the exact original surface. Nevertheless, let us note that Prados and Faugeras' framework allows to understand exactly what we compute, namely the SDVS (which coincides with the value function considered in particular by Dupuis and Oliensis [14]). In practice, we fix the height of the solution at the singular points and on the boundary of the image, when we know it, and we "send" these values to infinity when this information is not available (i.e., we impose a state constraint). Finally Prados and his coworkers prove that, with such constraints, there *exists* a *unique* SDVS of the SFS equations[11].

4 Numerical solutions by "Propagation and PDEs methods"

In section 2, we have shown that the SFS problem can be considered as that of solving a first order PDE. In this section, we consider the numerical SFS methods consisting in solving *directly* the *exact* SFS PDE. We call

[8] More precisely, the minima of $u - \varphi$, where φ is the adequate subsolution [32].

[9] Let us recall that we have assumed that $I(x) = cos(\mathbf{n}, \mathbf{L})$.

[10] i.e., in SFS, the photographed surface.

[11] With some weak adequate assumptions; see [32].

them "propagation and PDEs methods". These numerical methods do not make any linearizations (at the opposite of the linear methods; see [15] for a recent state of the art). Moreover, they do not introduce any biases in the equations contrary to the variational methods which, for example, add regularization or integrability terms. For more details about variational approaches in Shape From Shading, we refer the reader to Horn and Brooks' book [19] and to the survey of Durou and his coworkers [15] (and references therein).

4.1 Related work

The propagation and PDEs methods can be subdivided into two classes. The *"single-pass" methods* and the *iterative methods*. The main single-pass methods are: the method of *characteristic strips* (introduced by Horn [18]), the method of *propagation of the equal-height contours* (introduced by Bruckstein [7] and improved by Kimmel and Bruckstein [21]), the *fast marching* method (proposed by Sethian and Kimmel [39, 22]). Amongst the iterative methods let us cite in particular: the algorithm introduced by Rouy and Tourin [38] and its extensions by Prados and Faugeras [36, 34], the algorithms of Dupuis and Oliensis [14] based on the control theory and differential games, the algorithms of Falcone et al. [9] based on finite elements. Let us note that, at the exception of the work of Prados and Faugeras [34, 35], all these methods deal only with the Eikonal equation [18, 7, 38, 21, 39] or with the orthographic SFS with oblique light source [14, 9, 22, 36].

In spite of the multiplicity of these methods, we can prove that **they all compute approximations of the same solution.** In particular, the initial equal-height contours method of Bruckstein [7] is a variant of the method of the characteristic strips of Horn [18]. In [7], Bruckstein assumes that the initial curve is an equal-height contour. By imposing such special Dirichlet boundary conditions, he drops the Neumann boundary conditions required by the basic method of the characteristic strips (see [23] for a nice and rigorous study of these methods). Basically both above methods are Lagrangian methods that suffer from unstability and topological problems, see for example [30]. To alleviate these problems Kimmel and Bruckstein [21] propose to upgrade Bruckstein's method by using a Eulerian formulation of the problem. In other respects, the connection between the front propagation problems and the Hamilton Jacobi equations are well known. In particular, roughly speaking, it has beeb proved that the viscosity solution of the Hamilton Jacobi equation associated with a front propagation corresponds with the evolution of the initial contour defined by Huygens' principle; see for example [17]. In the same way, the other methods we cite above (Sethian's, Rouy-Tourin's, Dupuis-Oliensis', Falcone's and Prados-Faugeras' methods) compute some approximations of the viscosity solutions of the SFS equations. In particular in [40], Sethian and Vladimirsky

prove that the numerical solutions computed by the fast marching/ordered upwind methods converge toward the continuous viscosity solution (with Dirichlet boundary data on the boundary of the image). In [35], Prados and Faugeras generalize and unify the results proved in [38, 14, 9, 36, 34]. More precisely, they show that in all cases, the authors compute approximations of the SDVS. Basically, the difference between the work [38, 14, 9, 36, 34] is based on the choice of the boundary conditions; see [32]. In a general manner, all propagation and PDE methods require additional constraints: in particular, Dirichlet, Neumann or Soner boundary conditions. In other words, the computed solutions are characterized by the boundary conditions. These boundary conditions must contain enough information. Also, this information is thereby propagated "along" the solutions. Let us note that except for Horn's [18] and Bruckstein and Kimmel's method [7, 21], all the previous methods can deal with various Dirichlet/Soner boundary conditions. More precisely, the algorithms of Rouy and Tourin [38], Dupuis and Oliensis [14], Sethian [39] and Prados and Faugeras [36, 34] can use Dirichlet and/or Soner conditions on the boundary of the image $\partial\Omega$ at all the singular points $\mathcal{S}$ and on any other part of the image (for example, on an equal-height contour...). For instance, when we do not know the values of the solution at any points of the image, we can impose state constraints (i.e. Soner conditions) on $\partial\Omega \cup \mathcal{S}$ except for one point where we must impose a Dirichlet boundary condition. Contrary to these methods, let us note that Horn's [18] requires Dirichlet and Neumann boundary conditions and that Bruckstein's [7, 21] require the knowledge of an equal-height contour. This last constraint is a very specific Dirichlet condition and is much stronger than the previous ones. Note that implicitly, Bruckstein methods [7, 21] also impose state constraints on $\partial\Omega \cup \mathcal{S}$.

Finally, from a more numerical point of view, we can also remark that the approximation scheme considered by Sethian [39] is the one designed by Rouy and Tourin in [38]. Moreover, Prados and Faugeras' schemes are extensions of the Rouy and Tourin's scheme and their solutions coincide with those of Oliensis' schemes.

4.2 An example of provably convergent numerical method: Prados and Faugeras' method

In this section, we present the provably convergent numerical method of Prados and Faugeras [33]. Let us recall that this method unifies in particular the iterative methods of Rouy and Tourin [38], Prados et al. [36, 34] and Dupuis and Oliensis [14].

We consider here a finite difference approximation scheme. The reader unfamiliar with the notion of approximation schemes can refer to [3] or [33]. Let us just recall that, following [3], an approximation scheme is a functional

equation of the form

$$S(\rho, x, u(x), u) = 0 \qquad \forall x \in \overline{\Omega},$$

which "approximates" the considered PDE. S is defined on $\mathcal{M}\times\overline{\Omega}\times\mathbb{R}\times B(\overline{\Omega})$ into $\mathbb{R}$, $\mathcal{M} = \mathbb{R}^+ \times \mathbb{R}^+$ and $\rho = (h_1, h_2) \in \mathcal{M}$ defines the size of the mesh that is used in the corresponding numerical algorithms. $B(D)$ is the space of bounded functions defined on a set D.

Definition 1 *We say that a scheme S is stable*[12] *if for all fixed mesh size ρ it has solutions and if all the solutions are bounded independently of ρ.*

For ensuring the stability of a scheme, it is globally sufficient that it is monotonous (i.e. the function $u \mapsto S(\rho, x, t, u)$ is nonincreasing) and that the function $t \mapsto S(\rho, x, t, u)$ is nondecreasing, see [33]. For obtaining such a scheme, Prados and Faugeras [33] approximate the generic Hamiltonian H_g by

$$H_g(x, \nabla u(x)) \approx \sup_{a\in\bar{B}(0,1)} \left\{ \sum_{i=1}^{2} (-f_i(x,a)) \frac{u(x) - u(x + s_i(x,a)h_i\overrightarrow{e_i})}{-s_i(x,a)h_i} - l_g(x,a) \right\}$$

where $f_i(x,a)$ is the i^{th} component of $f_g(x,a)$ and $s_i(x,a)$ is its sign. Thus, they obtain the approximation scheme $S_{impl}(\rho, x, u(x), u) = 0$ with S_{impl} defined by:

$$S_{impl}(\rho, x, t, u) = \sup_{a\in\bar{B}(0,1)} \left\{ \sum_{i=1}^{2} (-f_i(x,a)) \frac{t - u(x + s_i(x,a)h_i\overrightarrow{e_i})}{-s_i(x,a)h_i} - l_g(x,a) \right\}.$$

By introducing a fictitious time $\Delta\tau$, they also transform this implicit scheme in a "semi-implicit" scheme (also monotonous):

$$S_{semi}(\rho, x, t, u) = t - \ (\ u(x) + \Delta\tau\ S_{impl}(\rho, x, u(x), u)\ ),$$

where $\Delta\tau = (f_g(x, a_0) \cdot (1/h_1, 1/h_2))^{-1}$; a_0 being the optimal control associated with $S_{impl}(\rho, x, u(x), u)$. Let us emphasize that these two schemes have exactly the same solutions and that they verify the previous monotonicity conditions (with respect to t and u). Prados and Faugeras prove in [33] the stability of these two schemes.
By construction, these two schemes are consistent[12] with the SFS equations as soon as the brightness image I is Lipschitz continuous; see [33]. Using the stability and the monotonicity of the schemes and some uniqueness results, it follows directly from [3] that the solutions of the approximation schemes S_{impl} and S_{semi} converge towards the unique viscosity solution of the considered equation (complemented with the adequate boundary conditions) when the mesh size vanishes; see [33].

[12] Following Barles and Souganidis definitions [3].

We now describe an *iterative algorithm* that computes numerical approximations of the solutions of a scheme $S(\rho, x, u(x), u) = 0$ for all fixed $\rho = (h_1, h_2)$. We denote, for $k \in \mathbb{Z}^2$, $x_k = (k_1 h_1, k_2 h_2)$, and $Q := \{k \in \mathbb{Z}^2$ s.t. $x_k \in \overline{\Omega}\}$. We call "pixel" a point x_k in $\overline{\Omega}$. Since $\overline{\Omega}$ is bounded the number of pixels is finite. The following algorithm computes for all $k \in Q$ a sequence of approximations U_k^n of $u(x_k)$:

Algorithm:

1. *Initialisation* ($n = 0$)*:* $\forall k \in Q,\ U_k^0 = u_0(x_k)$*;*
2. *Choice of a pixel* x_k *and modification (step* $n+1$*) of* U_k^n*: we choose* U^{n+1} *such that*

$$\begin{cases} U_l^{n+1} = U_l^n \quad \textit{if} \quad l \neq k, \\ S(\rho, x_k, U_k^{n+1}, U^n) = 0; \end{cases}$$

3. *Choose the next pixel* x_k *(using alternating raster scans [13]) and go back to 2.*

In [33], Prados and Faugeras prove that if u_0 is a supersolution of the SFS scheme S_{impl} (respectively, S_{semi}) then step 2 of the algorithm has always a unique solution and that the computed numerical solutions converge (when $n \to +\infty$) toward the solutions of the scheme. Many details about the implementation of the algorithm can be found in [33].

5 Examples of numerical results

In this section, we show some examples of numerical results on real images. In these experiments, we test the implicit generic SFS algorithm of Prados and Faugeras. At the same time, we suggest some *applications* of the SFS methods hoping that the results will convince the reader of the *applicability of this method to real problems.*

Let us recall that we have assumed that the camera is geometrically and photometrically calibrated. In the experiments of sections 5.1 and 5.2 we know the focal length (5.8 mm) and approximately the pixel size (0.0045 mm; CCD size = 1/2.7") of the digital camera (Pentax Optio 330GS). In section 5.3, we choose some arbitrary reasonable parameters. Let us note that in these tests, we also make some educated guesses for gamma correction (when the photometric properties of the images seem incorrect).

5.1 Document restoration using SFS

In this section, we consider a reprographic system to remove the geometric and photometric distortions generated by the classical photocopy of a bulky book. Note that several solutions have been proposed in the SFS literature. Let us cite in particular the work of Wada et al. [43], Cho et al. [10]

and Courteille et al. [11]. Here, the acquisition process we use is a classical camera. The book is illuminated by a single light source located at infinity or close to the optical center (following the models described in section 2). The acquired images are then processed using Prados and Faugeras' SFS method to obtain the shape of the photographed page. Let us emphasize that, for obtaining a compact experimental system, the camera must be located relatively close to the book. Therefore the *perspective model is especially relevant* for this application. Also, the distortion due to the perspective clearly appears in the image a) of figure 4. In this SFS method we assume that the albedo is constant. In this application, this does not

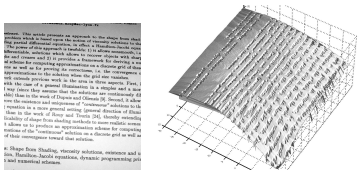

a) b)

FIGURE 3. a) Real image of a page of text [size $\simeq 800 \times 800$]; b) Surface recovered from a) by Prados and Faugeras' generic algorithm (without removing the printed parts of a)),

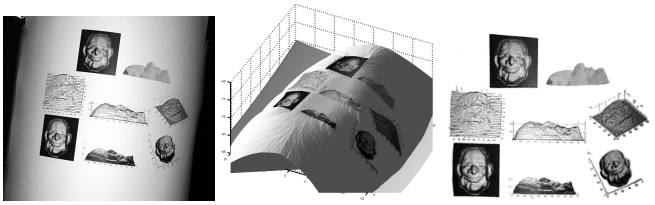

a) b) c)

FIGURE 4. a) real image of a page containing pictures and graphics [size $\simeq 2000 \times 1500$], b) surface (textured by the printed parts of a)) recovered from a) by Prados and Faugeras' generic algorithm (after having removed and inpainted the ink parts of a)). c) An orthographic projection of the surface b): the geometric (and photometric) distorsions are significantly reduced.

hold because of the printed parts. Before recovering the surface of the page, we therefore localize the printed parts by using image statistic (similar to Cho's [10]) and we erase them automatically by using an inpainting algorithm. This step can produce an important pixel noise. Nevertheless, this is not a problem for us because, as figure 3-b) shows, *Prados and Faugeras' SFS method is extremely robust to pixel noise*: figure 3-b) displays the result produced by this algorithm (after 10 iterations) using the image of a text page with its pigmented parts, Fig.3-a). In this test, characters are considered as noise. Once we have recovered the three-dimensional shape of the page, we can then flatten the surface. Note that at each step of this

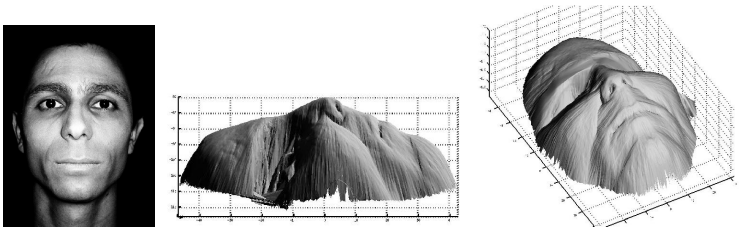

a) b) c)

FIGURE 5. a) Real face image [size $\simeq 450 \times 600$]; b) surface recovered from a) by the generic SFS algorithm with the perspective model with the light source located at the optical center; c) surface recovered by the generic SFS algorithm with the same modeling hypotheses as for b) after the inpainting process.

restoration process we can keep the correspondences with the pixels in the image. Thus, at the final step, we can restore the printed parts.
To prove the applicability of this method, we have tested it on a page wrapped on a cylindrical surface[13] (we have used a cheap camera and flash in an approximately dark room). Figure 4 shows the original image in a), the reconstructed surface (after 10 iterations) (textured by the ink parts of a)) in b) and an orthographic projection of the reconstructed surface, in e). Figure 4-c) indicates that this method allows to remove the perspective and photometric distortions.

5.2 Face reconstruction from SFS

In this section we propose a very simple protocol based on SFS for face reconstruction. We use one camera equiped with a basic flash in an approximately dark place. We have tested the implicit generic SFS algorithm on a real image of a face (using a small amount of make-up to make it more Lambertian) located at $\simeq$700 mm of the camera in an approximately dark place (see Fig.5-a)). Figure 5-b) shows the surface recovered by the generic algorithm with the perspective model with a point light source at the optical center. As in the previous application, the albedo is not constant over the whole image. Therefore we removed[14] the eyes and the eyebrows in the image by using an inpainting algorithm. Figure 5 shows in c) the surface recovered from the image obtained after the inpainting process.

5.3 Potential applications to medical images

In this section, we are interested in applying the SFS method to some medical images. Our interest is motivated, for example, by the work of Craine

[13] For emphasizing the perspective effect.
[14] Can be automated by matching the image to a model image already segmented.

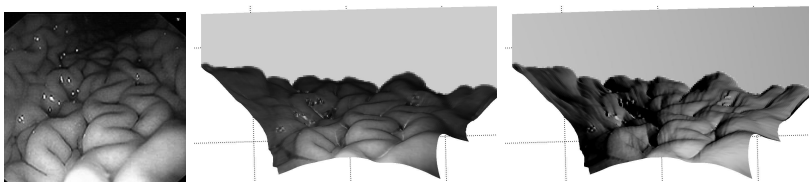

a) b) c)

FIGURE 6. Reconstruction of a normal stomach. a) Original image of a normal stomach [size$\simeq 200 \times 200$]; b) surface recovered from a) by the generic SFS algorithm with the perspective model with the light source located at the optical center; c) surface b) visualized with a different illumination.

et al. [12] (who use SFS for correcting some errors on the quantitative measurement of areas in the cervix, from colonoscopy images). We have applied Prados and Faugeras' algorithm to an endoscopic image of a normal stomach[15] (see figure 6-a)). For producing such an image, the light source must be very close to the camera, because of space constraints. So the adequate modeling is that of the "perspective SFS" with the light source located at the optical center. In figure 6-b), we show the result obtained. To further show the quality of the reconstruction, we display the surface b) with a different illumination. Finally, notice that the stomach wall is not perfectly Lambertian (see Fig.6-a)). This suggests the robustness of this SFS method to departures from the Lambertian hypothesis.

6 Conclusion

After having presented the SFS problem, we have described its main difficulties: in practice, the classical SFS equations are ill-posed. In a second time, we have focused on the numerical methods. We have considered the propagation and PDEs methods; in particular Prados and Faugeras' methods. We have demonstrated the applicability of the SFS methods by displaying some experimental results with real images. Finally, we have suggested that SFS may be useful in a number of real-life applications.

7 References

[1] S. Bakshi and Y. Yang. Shape from shading for non-lambertian surfaces. In *ICIP'94*, volume 94, pages 130–134, 1994.

[2] G. Barles. *Solutions de Viscosit des Equations de Hamilton–Jacobi.* Springer–Verlag, 1994.

[15] Suggested by Tankus and Sochen [42]; http://www.gastrolab.net/

[3] G. Barles and P. Souganidis. Convergence of approximation schemes for fully nonlinear second order equations. *Asymptotic Analysis*, 4:271–283, 1991.

[4] P. N. Belhumeur, D. J. Kriegman, and A. L. Yuille. The bas-relief ambiguity. *IJCV*, 35(1):33–44, 1999.

[5] M. Brooks. Two results concerning ambiguity in shape from shading. In *AAAI-83*, pages 36–39, 1983.

[6] M. Brooks, W. Chojnacki, and R. Kozera. Shading without shape. *Quarterly of Applied Mathematics*, 50(1):27–38, 1992.

[7] A. M. Bruckstein. On shape fron shading. *Computer Vision Graphics Image Process*, 44:139–154, 1988.

[8] A. Bruss. The eikonal equation: Some results applicable to computer vision. *Journal of Mathematical Physics*, 23(5):890–896, 1982.

[9] F. Camilli and M. Falcone. An approximation scheme for the maximal solution of the shape-from-shading model. In *ICIP'96*, pages 49–52, 1996.

[10] S. Cho and H. Saito. A Divide-and-Conquer Strategy in Shape from Shading problem. In *CVRP'97*, 1997.

[11] F. Courteille, A. Crouzil, J.-D. Durou, and P. Gurdjos. Towards shape from shading under realistic photographic conditions. In *ICPR'04*, 2004.

[12] B. Craine, C. E.R., C. O'Toole, and Q. Ji. Digital imaging colposcopy: Corrected area measurements using Shape-from-Shading. *IEEE Transactions on Medical Imaging*, 17(6):1003–1010, 1998.

[13] P.-E. Danielsson. Euclidean Distance Mapping. *Computer Graphics and Image Processing*, 14(3):227–248, 1980.

[14] P. Dupuis and J. Oliensis. An optimal control formulation and related numerical methods for a problem in shape reconstruction. *The Annals of Applied Probability*, 4(2):287–346, 1994.

[15] J.-D. Durou, M. Falcone, and M. Sagona. A survey of numerical methods for shape from shading. Technical Report 2004-2-R, IRIT, 2004.

[16] J.-D. Durou and D. Piau. Ambiguous shape from shading with critical points. *JMIV*, 12(2):99–108, 2000.

[17] L. Evans and P. Souganidis. Differential games and representation formulas for solutions of hamilton-jacobi-isaacs equations. *Indiana Univ. Math. J.*, 33:773–797, 1984.

[18] B. Horn. Obtaining shape from shading information. In P. Winston, editor, *The Psychology of Computer Vision*. McGraw-Hill, New York, 1975.

[19] B. Horn and M. Brooks, editors. *Shape from Shading*. The MIT Press, 1989.

[20] R. Kimmel and A. Bruckstein. "Global shape-from-shading". *CVGIP: Image Understanding*, pages 360–369, 1995.

[21] R. Kimmel and A. Bruckstein. Tracking level sets by level sets : A method for solving the shape from shading problem. *Computer Vision and Image Understanding*, 62(2):47–58, 1995.

[22] R. Kimmel and J. Sethian. Optimal algorithm for shape from shading and path planning. *JMIV*, 14(2):237–244, 2001.

[23] R. Klette, R. Kozera, and K. Schlüns. Shape from shading and photometric stereo methods. Technical Report CITR-TR-20, University of Auckland, New Zealand, 1998.

[24] R. Kozera. Uniqueness in shape from shading revisited. *JMIV*, 7:123–138, 1997.

[25] K. Lee and C. Kuo. Shape from shading with a generalized reflectance map model. *CVIU*, 67(2):143–160, 1997.

[26] P.-L. Lions, E. Rouy, and A. Tourin. Shape-from-shading, viscosity solutions and edges. *Numer. Math.*, 64:323–353, 1993.

[27] T. Okatani and K. Deguchi. On classification of singular points for global shape from shading. In *ACCV'98*, volume 1351, pages 48–55, 1998.

[28] J. Oliensis. Shape from shading as a partially well–constrained problem. *CVGIP: Image Understanding*, 54(2):163–183, 1991.

[29] J. Oliensis. Uniqueness in shape from shading. *IJCV*, 2(6):75–104, 1991.

[30] S. Osher and J. Sethian. Fronts propagating with curvature dependent speed: algorithms based on the Hamilton–Jacobi formulation. *Journal of Computational Physics*, 79:12–49, 1988.

[31] A. Pentland. Local shading analysis. *PAMI*, 6:170–187, 1984.

[32] E. Prados, F. Camilli, and O. Faugeras. A viscosity method for Shape-From-Shading without boundary data. Technical Report RR-5296, INRIA, 2004.

[33] E. Prados and O. Faugeras. A mathematical and algorithmic study of the lambertian SFS problem for orthographic and pinhole cameras. Technical Report RR-5005, INRIA, 2003.

[34] E. Prados and O. Faugeras. "Perspective Shape from Shading" and viscosity solutions. In *ICCV'03*, volume 2, pages 826–831, 2003.

[35] E. Prados and O. Faugeras. Unifying approaches and removing unrealistic assumptions in Shape from Shading: Mathematics can help. In *ECCV'04*, 2004.

[36] E. Prados, O. Faugeras, and E. Rouy. Shape from shading and viscosity solutions. In *ECCV'02*, volume 2351, pages 790–804, 2002.

[37] H. Ragheb and E. Hancock. A probabilistic framework for specular shape-from-shading. *Pattern Recognition*, 36:407–427, 2003.

[38] E. Rouy and A. Tourin. A Viscosity Solutions Approach to Shape-from-Shading. *SIAM J. of Numerical Analysis*, 29(3):867–884, 1992.

[39] J. Sethian. *Level Set Methods*. Cambridge University Press, 1996.

[40] J. Sethian and A. Vladimirsky. Ordered upwind methods for static hamilton–jacobi equations: Theory and algorithms. *SIAM J. of Numerical Analysis*, 41(1):325–363, 2003.

[41] A. Tankus, N. Sochen, and Y. Yeshurun. A new perspective [on] Shape-from-Shading. In *ICCV'03*, volume 2, pages 862–869, 2003.

[42] A. Tankus, N. Sochen, and Y. Yeshurun. Reconstruction of medical images by perspective Shape-from-Shading. In *ICPR'04*, 2004.

[43] T. Wada, H. Ukida, and T. Matsuyama. Shape from shading with interreflections under proximal light source-3D shape reconstruction of unfolded book surface from a scanner image. In *ICCV'95*, 1995.